JACS
JOURNAL OF THE AMERICAN CHEMICAL SOCIETY

Article

pubs.acs.org/JACS

Exploiting Metalloporphyrins for Selective Living Radical Polymerization Tunable over Visible Wavelengths

Sivaprakash Shanmugam,[†] Jiangtao Xu,*[,†,‡] and Cyrille Boyer*[,†,‡]

[†]Centre for Advanced Macromolecular Design (CAMD), School of Chemical Engineering, UNSW Australia, Sydney, New South Wales 2052, Australia

[‡]Australian Centre for NanoMedicine, School of Chemical Engineering, UNSW Australia, Sydney, New South Wales 2052, Australia

Supporting Information

ABSTRACT: The use of metalloporphyrins has been gaining popularity particularly in the area of medicine concerning sensitizers for the treatment of cancer and dermatological diseases through photodynamic therapy (PDT), and advanced materials for engineering molecular antenna for harvesting solar energy. In line with the myriad functions of metalloporphyrins, we investigated their capability for photoinduced living polymerization under visible light irradiation over a broad range of wavelengths. We discovered that zinc porphyrins (i.e., zinc tetraphenylporphine (ZnTPP)) were able to selectively activate photoinduced electron transfer–reversible addition–fragmentation chain transfer (PET-RAFT) polymerization of trithiocarbonate compounds for the polymerization of styrene, (meth)acrylates and (meth)acrylamides under a broad range of wavelengths (from 435 to 655 nm). Interestingly, other thiocarbonylthio compounds (dithiobenzoate, dithiocarbamate and xanthate) were not effectively activated in the presence of ZnTPP. This selectivity was likely attributed to a specific interaction between ZnTPP and trithiocarbonates, suggesting novel recognition at the molecular level. This interaction between the photoredox catalyst and trithiocarbonate group confers specific properties to this polymerization, such as oxygen tolerance, enabling living radical polymerization in the presence of air and also ability to manipulate the polymerization rates (k_p^{app} from 1.2–2.6 × 10^{-2} min^{-1}) by varying the visible wavelengths.

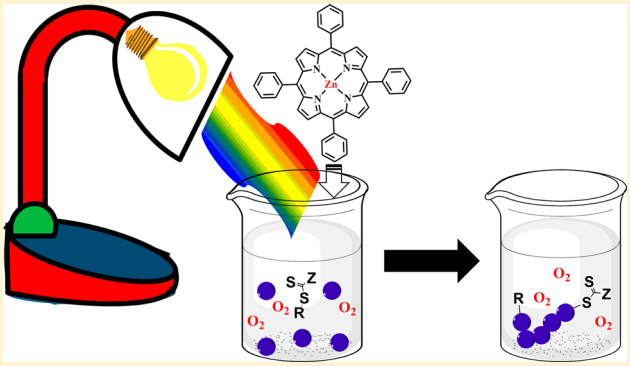

INTRODUCTION

Molecular recognition plays an integral role in biology especially in biomolecular interactions involving enzyme catalysis, cellular signaling, protein–protein interaction, reactant transport, noncovalent receptor binding and DNA hybridization.[1] In these processes, recognition of two or more molecular binding partners can lead to their association or to their rejection,[2] which governs several important biologic processes. For instance, the molecular recognition between DNA and specific proteins activates and controls the rate of transcription of genetic information from DNA to mRNA, i.e., the polymerization of RNA, and subsequently the polymerization of protein. Because of these applications, in recent years, researchers have developed numerous artificial systems for molecular and macroscopic recognition involving the use of simple interactions such as hydrogen bonds, $\pi-\pi$ stacking, entropic depletion, and capillary forces.[3] However, molecular recognition to specifically activate and deactivate a synthetic living radical polymerization, such as atom transfer radical polymerization (ATRP),[4] nitroxide-mediated polymerization (NMP)[5] and reversible addition–fragmentation chain transfer polymerization (RAFT)[6] has not been explored.

In this study, we have investigated different transition metal porphyrins to access their suitability as photoredox catalysts for the activation of photoinduced electron transfer–reversible addition–fragmentation chain transfer (PET-RAFT) polymerization (Scheme 1). Although metalloporphyrins have generated great interests due to their applications in phototherapy and photovoltaics,[7] they have never been employed as photoredox catalysts to activate a chemical reaction such as living radical polymerization (in the exception of some specific polymerizations mediated by cobalt-porphyrin[8−11] and chlorophyll[12]). By evaluating the efficiency of different metalloporphyrins in the PET-RAFT process, we discovered selective activation of trithiocarbonates over other thiocarbonylthio compounds (dithiobenzoate, dithiocarbamate and xanthate) in the presence of the zinc porphyrin. This is a novel form of molecular recognition involving the specific interaction of zinc porphyrin and trithiocarbonates. Zinc and sulfur interaction play a critical role at the cellular level; this partnership generates redox-active coordination environments for the redox-inert zinc ion to enable protein motifs such as zinc fingers to carry out functions such as DNA recognition for transcriptional activation.[13] In our study, we were able to introduce a similar form of recognition with zinc tetraphenylporphine (ZnTPP)

Received: May 21, 2015
Published: July 13, 2015

DOI: 10.1021/jacs.5b05274
J. Am. Chem. Soc. 2015, 137, 9174–9185

Scheme 1. Proposed Mechanism for Photoinduced Electron Transfer−Reversible Addition−Fragmentation Chain Transfer (PET-RAFT) Polymerization Mediated by ZnTPP and Different Thiocarbonylthio Compounds[a]

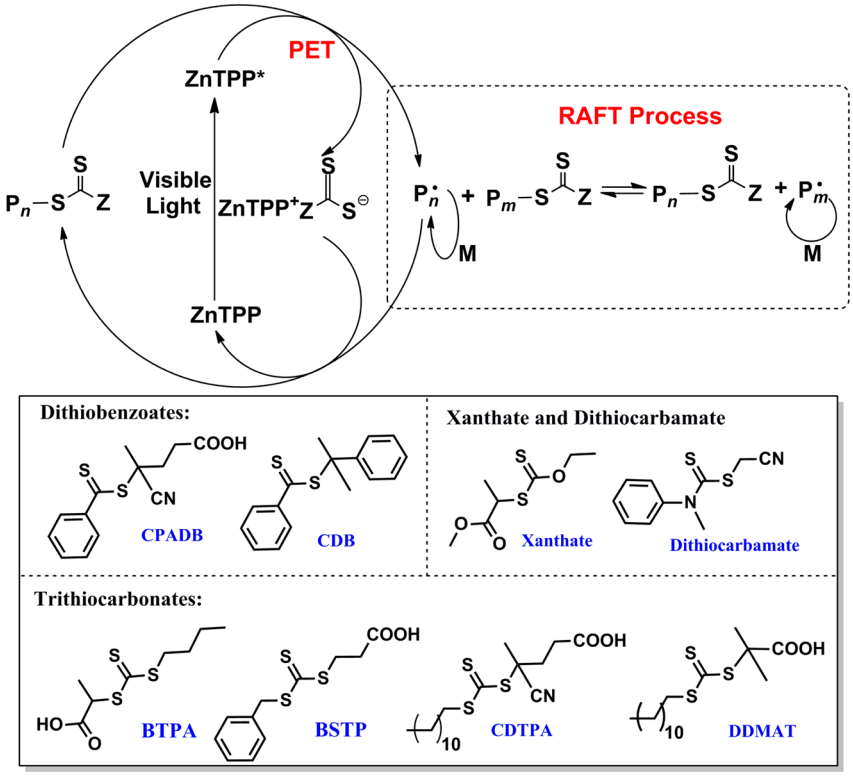

[a]4-Cyanopentanoic acid dithiobenzoate (CPADB), cumyl benzodithioate (CDB), 2-(*n*-butyltrithiocarbonate)-propionic acid (BTPA), 3-benzylsulfanyl thiocarbonylthiosulfanyl propionic acid (BSTP), 4-cyano-4-[(dodecylsulfanylthiocarbonyl) sulfanyl] pentanoic acid (CDTPA), 2-(dodecylthiocarbonothioylthio)-2-methylpropionic acid (DDMAT), cyanomethyl methyl(phenyl) carbamodithioate (dithiocarbamate), and methyl 2-[(ethoxycarbonothioyl)sulfanyl]propanoate (xanthate).

where activation of trithiocarbonate leads to efficient polymerization while activation of dithiobenzoate is sluggish, leading to a much slower and inefficient polymerization. In contrast to our previous studies using transition metal,[14−17] organic[18] and biophotoredox catalysts,[12,19] such selectivity for a specific thiocarbonylthio compound had not been observed before. According to our proposed PET-RAFT mechanism (Scheme 1),[14] the redox potential of thiocarbonylthio compound should be higher than the reduction potential of the photoredox catalyst for successful initiation. To be specific, the polymerization of acrylates with trithiocarbonates (i.e., 2-(*n*-butyltrithiocarbonate)-propionic acid (BTPA)) requires strong reducing agents to activate the PET-RAFT process, while polymerization of methacrylates with dithiobenzoates (i.e., 4-cyanopentanoic acid dithiobenzoate (CPADB)) is successful using less powerful reducing agents due to the difference in redox potential between these two species (−0.6 V versus −0.4 V, potential versus standard calomel electrode (SCE), for BTPA and CPADB respectively).[12,14−18] However, the ZnTPP investigated in this study is an exception to this rule as the activation of trithiocarbonate is carried out more efficiently than dithiobenzoate.

In addition, the polymerization activated by ZnTPP presents more unique properties in comparison to those activated by copper,[20−35] iridium,[14,36−39] ruthenium,[17,40−42] and other photoredox catalysts[12,18,43−50] due to this specific interaction. For instance, the polymerization of MA fully open to air was achieved with a living character. Most of reversible-deactivation radical polymerization techniques are sensitive to the presence of oxygen as propagating radicals are rapidly trapped by oxygen. For activators generated by electron transfer-ATRP (AGET),[24,51,52] single electron transfer−living radical polymerization (SET-LRP),[53−57] photoinduced ATRP[24,58,59] and PET-RAFT using an *fac*-[Ir(ppy)$_3$] and Ru(bpy)$_3$Cl$_2$,[14,16] the oxygen can be consumed or reduced during an inhibition period prior to polymerization. In the case of PET-RAFT activated by ZnTPP, the polymerization was activated under air without (or very short) an inhibition period. This result is attributed to possible coordination of ZnTPP to the trithiocarbonate, allowing an activation and deactivation of the polymerization in the presence of oxygen. Another unique property of ZnTPP is the possibility to carry out the polymerization at different wavelengths (from 435 to 655 nm). Indeed, most of the photoredox catalysts, except chlorophyll,[12] can activate a living radical polymerization under a specific wavelength, which is usually centered on the high energy visible region of spectrum, i.e., blue and UV region.[14,17,18,20−32,34−50,60−77] The use of high energy wavelength considerably reduces the potential applications of photoinduced living polymerization in biological material science, as organic compounds strongly absorb light with the wavelength lower than 450 nm. In the literature, we could only find few reports[78−86] of uncontrolled photopolymerization using wavelengths above 550 nm. ZnTPP presents absorptions at 520, 570, and 600 nm, which can be used to activate a PET-RAFT polymerization. More importantly, the polymerization rate is easily manipulated according to the wavelengths employed in the case of ZnTPP, which has never been reported in photoinduced living polymerization.

DOI: 10.1021/jacs.5b05274
J. Am. Chem. Soc. 2015, 137, 9174−9185

Scheme 2. Different Porphyrin Structures Investigated in This Study[a]

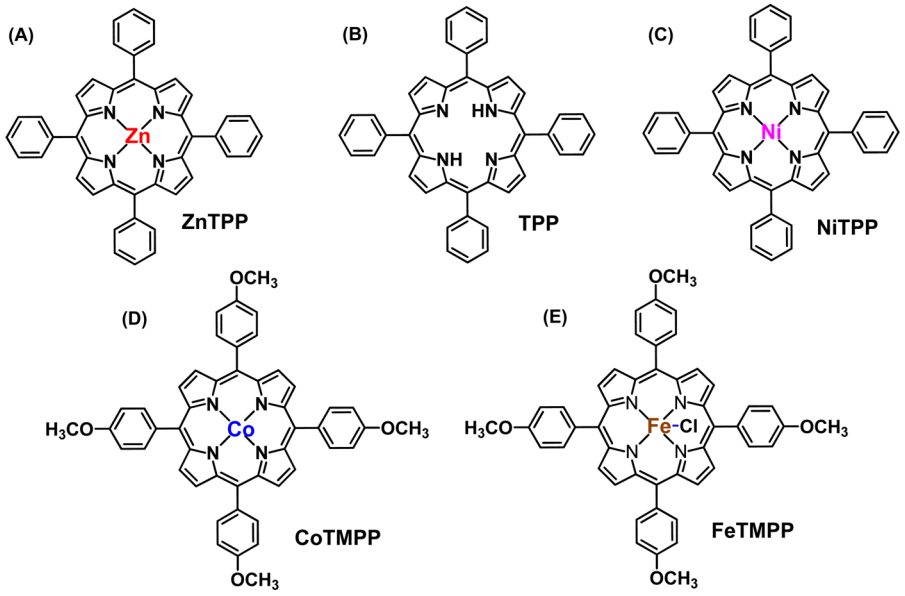

[a]5,10,15,20-Tetraphenyl-21*H*,23*H*-porphine zinc (ZnTPP, A), *meso*-tetraphenylporphyrin (TPP, B), 5,10,15,20-tetraphenyl-21*H*,23*H*-porphine nickel(II) (NiTPP, C), 5,10,15,20-tetrakis(4-methoxyphenyl)-21*H*,23*H*-porphine cobalt(II) (CoTMPP, D), and 5,10,15,20-tetrakis(4-methoxyphenyl)-21*H*,23*H*-porphine iron(III) chloride (FeTMPP, E).

Table 1. Screening Porphyrin Based Photoredox Catalysts for Living Radical Polymerization[a]

#	photocatalyst	monomer	RAFT	[ZnTPP]/[M] (ppm)	time (h)	α (%)[b]	$M_{n,th.}$[c] (g/mol)	$M_{n,GPC}$[d] (g/mol)	M_w/M_n
1	TPP	MMA	CPADB	100	24	55	11 240	11 440	1.10
2	TPP	MA	BTPA	100	6	13.5	–	–	–
3	ZnTPP	MMA	CPADB	100	24	25	6080	5640	1.19
4	ZnTPP	MMA	CDB	100	24	2	–	–	–
5	ZnTPP	MMA	CDTPA	100	12	90	21 900	21 050	1.14
6	ZnTPP	MMA	CDTPA	50	12	50	11 650	10 940	1.12
7	ZnTPP	MMA	DDMAT	50	12	74	15 240	40 721	1.9
8	ZnTPP	MA	BTPA	100	2	80	13 140	12 700	1.09
9	FeTMPP	MMA	CPADB	100	24	0	–	–	–
10	FeTMPP	MA	BTPA	100	6	4.5	–	–	–
11	CoTMPP	MMA	CPADB	100	24	0	–	–	–
12	CoTMPP	MA	BTPA	100	6	5	–	–	–
13[b]	NiTPP	MMA	CPADB	100	24	0	–	–	–
14[b]	NiTPP	MA	BTPA	100	6	5	–	–	–

[a]Experimental conditions: [Monomer]:[RAFT]:[Catalyst] = 200:1:2 × 10^{-2} (100 ppm) or 200:1:1 × 10^{-2} (50 ppm); solvent DMSO; light source 5 W red LED light (λ_{max} = 635 nm). [b]The solvent is *N*-methyl-2-pyrrolidone (NMP) due to the poor solubility of NiTPP. [c]Theoretical molecular weight was calculated using the following equation: $M_{n,th.} = [M]_0/[RAFT]_0 \times MW^M \times \alpha + MW^{RAFT}$, where $[M]_0$, $[RAFT]_0$, MW^M, α, and MW^{RAFT} correspond to initial monomer concentration, initial RAFT concentration, molar mass of monomer, conversion determined by ^{1}H NMR, and molar mass of RAFT agent. [d]Molecular weight and polydispersity index were determined by GPC analysis (DMAc as eluent) calibrated to polystyrene standard. (−): not determined.

Indeed, in most of previous photoactivated polymerization techniques,[36,37,45,60,61,87] the polymerization rates could be steadily manipulated by light intensity and/or catalyst concentration, but rarely using different wavelengths with a single photoredox catalyst.

RESULTS AND DISCUSSION

1. Screening Metalloporphyrins as Photoredox Catalysts to Activate Living Radical Polymerization under Light. Porphyrin is an important functional molecule, which contains four pyrrole units linked by four carbon atoms in a planar arrangement with an 18π distinct aromatic character.[88,89] Porphyrins and their derivatives have received great interest in the last 30 years[90] due to their numerous applications in organic reactions,[91] energy conversion (photovoltaic),[92,93] photonics[94] and medicine (photodynamic therapy).[95] In the early 90s, porphyrin compounds have been employed as catalysts to conduct living anionic polymerization.[96−98] Later, Matyjaszewski,[99] Bruns[100] and co-workers demonstrated the use of heme as catalyst to mediate ATRP. However, these compounds have not been investigated as potential photoredox catalysts to activate a (living) radical polymerization under light. In this study, five porphyrin based photoredox catalysts, 5,10,15,20-tetraphenyl-21*H*,23*H*-porphine zinc (ZnTPP, Scheme 2A), *meso*-tetraphenylporphyrin (TPP, Scheme 2B), 5,10,15,20-tetraphenyl-21*H*,23*H*-porphine nickel(II) (NiTPP,

DOI: 10.1021/jacs.5b05274
J. Am. Chem. Soc. 2015, 137, 9174−9185

Scheme 2C), 5,10,15,20-tetrakis(4-methoxyphenyl)-21*H*,23*H*-porphine cobalt(II) (CoTMPP, Scheme 2D), and 5,10,15,20-tetrakis(4-methoxyphenyl)-21*H*,23*H*-porphine iron(III) chloride (FeTMPP, Scheme 2E) were investigated to selectively activate thiocarbonylthio compounds for the living radical polymerization of methacrylates and acrylates.

As the porphyrins absorb intensely in the Soret region (around 430 nm) and partially in the Q region (around 600 nm),[101] we carried out all the initial polymerization tests under blue LED light (435−480 nm) (SI, Table S1) and under red light (610−655 nm) (Table 1) using methyl acrylate (MA) and methyl methacrylate (MMA). For MMA polymerization in the presence of 4-cyanopentanoic acid dithiobenzoate (CPADB), TPP and ZnTPP gave low monomer conversions (Table 1, #1 and #3, 55% for TPP and 25% for ZnTPP) after 24 h under red light exposure, while the polymerizations conducted with other metalloporphyrins showed negligible conversions (Table 1, #9, #11 and #13). Another dithiobenzoate (cumyl dithiobenzoate, CDB) presented an even lower conversion (2%) using ZnTPP as catalyst (Table 1, #4). Interestingly, the polymerization of MMA in the presence of ZnTPP appears to be relatively low in comparison to those mediated by other metal photoredox catalysts, such as *fac*-[Ir(ppy)$_3$] and Ru(bpy)$_3$Cl$_2$, which generally provided >80% conversion after 24 h light exposure. Surprisingly, in the case of MA polymerization, ZnTPP uniquely presented greater catalytic activity to activate BTPA as high monomer conversion was observed (93% and 80% under blue and red light, respectively).

Depending on the metal ions in the core of the porphyrins, different catalytic activity for the polymerization of MMA and MA were displayed. The difference in the catalytic activity was attributed to their photophysical properties upon excitation. Unlike Ni^{2+}, Co^{2+} and Fe^{3+} core, the Zn^{2+} atom in the tetraphenylporphyrin exhibited very little charge-transfer interaction between the metal and the π-conjugated system in the excited state, and therefore, the absorption spectra are assigned only to $\pi-\pi^*$ transitions. In contrast, under light, there is considerable triplet state formation for both ZnTPP (Φ_T = 0.88) and TPP (Φ_T = 0.82) with the fluorescence quantum yield slightly lower in ZnTPP (Φ_F = 0.04) than the TPP (Φ_F = 0.13) (Table 2). In addition, decay of the excited singlet state of both ZnTPP and TPP leads to the population of the triplet levels; consequently, the decrease in fluorescence quantum yield can be associated with an increase in the rate constant for intersystem crossing.[102−104] The ability of ZnTPP and TPP to stay longer in the excited state increases the probability for photoinduced electron transfer to take place from the excited π-conjugated porphyrin to the RAFT agents which leads to radical generation and initiation of polymerization. This result appears consistent with our previous observations for organophotoredox catalysts where a longer excited state is associated with a more efficient activation of PET-RAFT.[17] Furthermore, energy loss due to internal conversion for both ZnTPP and TPP can be neglected as the sum of Φ_F and Φ_T is close to unity.[102]

Table 2. Photophysical Data for Metalloporphyrins[102−104]

#	photoredox catalyst	$\Phi_F{}^a$	$\tau_F{}^a$	$\Phi_T{}^a$	k_{isc}/s^{-1a}
1	TPP	0.13	13.6	0.82	4.7×10^7
2	ZnTPP	0.04	2.7	0.88	3.6×10^8
3	NiTPP	$<10^{-4}$	–	–	$>10^{10}$

[a] Φ_F, Φ_T, τ_F and k_{isc}/s^{-1} correspond to fluorescence quantum yield, triplet quantum yield, fluorescence lifetime and rate constant for intersystem crossing, respectively.

In comparison to ZnTPP and TPP, NiTPP has a much lower fluorescence quantum yield and higher rate constant for intersystem crossing (Table 2). However, it is inefficient in its role to initiate PET-RAFT polymerization as it loses most of its excitation energy to rapid internal conversion from the lowest energy $\pi-\pi^*$ excited singlet state to a low-lying (*dd*) singlet state. The lack of long-lived NiTPP excited species is further supported by the fact that no observable luminescence could be measured due to nonradiative decay of the excited singlet state through internal conversion or intersystem crossing to a nonradiative triplet state.[102] Although there are limited examples in the literature that has looked into the photophysical properties of CoTMPP and FeTMPP, the inability of these porphyrins to initiate RAFT polymerization can be drawn from previous studies with the inefficiency is most likely due to the paramagnetic transition metal rather than the porphyrin core.[105] In previous reports, the presence of paramagnetic metals such as Fe^{3+} and Co^{2+} led to the enhancement of spin−orbital interactions which increased triplet state yield by radiationless transition from the excited singlet state and shortened the lifetime of radiative transition between the ground and triplet state. The shortened lifetime of the triplet state reduces the probability for electron transfer to take place between RAFT agents and iron and cobalt porphyrins leading to the absence of activation, and subsequent polymerization.[103,104,106]

2. Selective Activation of Trithiocarbonate under Visible Light. It is worth to note that ZnTPP showed greater ability to activate BTPA for MA polymerization than CPADB for MMA polymerization. This is not a common phenomenon. In our previous studies,[12,14−18] we have demonstrated that CPADB is easily activated as it presents a higher reduction potential (−0.4 V versus SCE) than BTPA (−0.6 V versus SCE). However, ZnTPP investigated in this study is an exception to this rule as activation of BTPA is carried out more efficiently than CPADB, which suggests an unusual selectivity possibly due to an interaction between ZnTPP and BTPA. As both ZnTPP and TPP have very similar properties, i.e., reduction potential ($\sim -(1.0-1.3)$ V vs SCE)[107] and high triplet quantum yield (Table 2), it was expected that both photoredox catalysts should be able to initiate BTPA. However, this hypothesis was incorrect as polymerization of MA in the presence of TPP was observed to be less efficient (13.5%, Table 1, #2). The discrepancy in the polymerization rates can be attributed to the coordination of zinc to the thiocarbonylthio moiety on RAFT which may lead to higher efficiency of PET-RAFT activation. Indeed, previous reports suggest that ZnTPP presents strong affinity to pyridine, thiol and trithiocarbonate.[108] To clarify this finding, we have performed UV−visible spectroscopy of ZnTPP, ZnTPP/BTPA (SI, Figure S1) and ZnTPP/CPADB (SI, Figure S1) before and after light irradiation. In the presence of BTPA and ZnTPP, we observed a new signal at 620 nm, while the signals of ZnTPP/CPADB did not change. This new signal at 620 nm is attributed to a possible interaction of trithiocarbonate with ZnTPP. In the case of other metalloporphyrins such as TPP, NiTPP, FeTMPP, and CoTMPP, the UV−vis spectra for the samples prepared under identical conditions displayed no change in signals before and after light irradiation (SI, Figure S2). Additionally, Kamigaito and co-workers exploited the specific interaction between

DOI: 10.1021/jacs.5b05274
J. Am. Chem. Soc. 2015, 137, 9174−9185

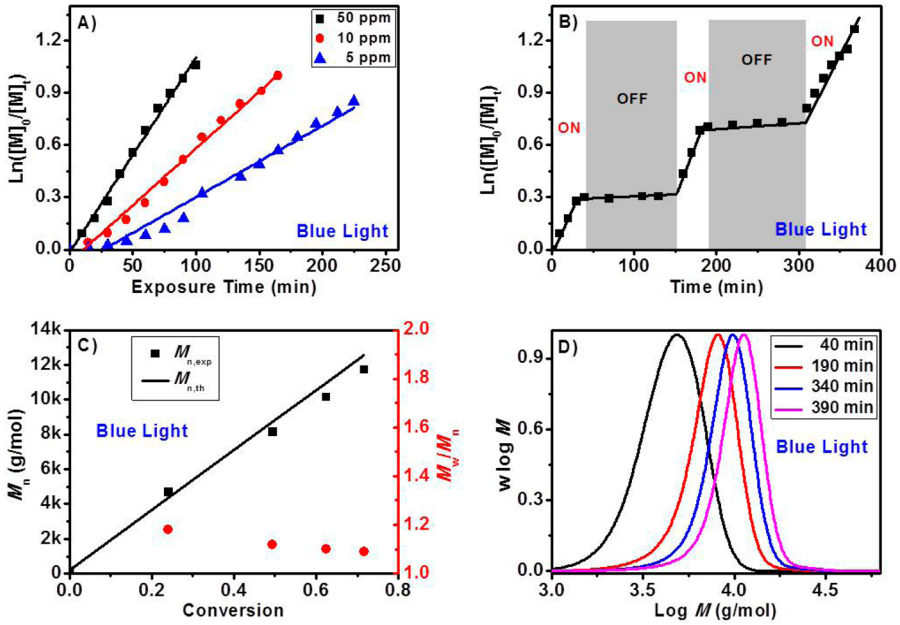

Figure 1. Online Fourier transform near-infrared (FTNIR) measurement for kinetic study of PET-RAFT polymerization of MA in the absence of oxygen at room temperature with ZnTPP as photoredox catalyst under blue light irradiation with BTPA as the chain transfer agent, using molar ratio of [MA]:[BTPA] = 200:1 in DMSO. (A) Plot of $\ln([M]_0/[M]_t)$ vs exposure time at different catalyst concentrations (50, 10, 5 ppm relative to monomer concentration); (B) "ON/OFF" online FTIR kinetics for 50 ppm relative to monomer concentration; (C) M_n vs conversion; and (D) molecular weight distributions at different time points for 50 ppm catalyst concentration.

trithiocarbonate and a Lewis acid, i.e., zinc (Zn^{2+}), to mediate a living cationic polymerization.[109−111]

To confirm that the behavior observed with BTPA is not dependent on the nature of monomer, i.e., MA, we decided to polymerize methyl methacrylate using 4-cyano-4-[(dodecylsulfanylthiocarbonyl) sulfanyl] pentanoic acid (CDTPA) and 2-(dodecylthiocarbonothioylthio)-2-methylpropionic acid (DDMAT) as thiocarbonylthio compounds, a group of trithiocarbonates capable of controlling methacrylates. The polymerization was only carried out under red LED light. As we showed in our previous studies,[112] CDTPA and DDMAT were able to undergo photolysis and generate radicals to initiate RAFT polymerization without the need of a photoredox catalyst in the presence of blue and green lights. However, in the presence of red light, no photolysis was observed leading to the conclusion that self-initiation was not possible at this wavelength.[112] In comparison with CPADB (Table 1, #3), much higher monomer conversions were observed for CDTPA (Table 1, #5 and 6) and DDMAT (Table 1, #7). These results support our hypothesis, which likely attributes to the specific activation of trithiocarbonate by ZnTPP through the coordination of trithiocarbonate with ZnTPP.

3. Polymerization under Blue Light Irradiation Catalyzed by ZnTPP. As ZnTPP shows a strong Soret band absorption at 420 nm in DMSO, the polymerization kinetics of MA was initially investigated in detail under blue light (λ_{max} = 460 nm) using various concentrations of catalyst (5, 10, and 50 ppm) with an online Fourier transform near-infrared (FTNIR) spectrometer to determine the monomer conversion and the presence or absence of inhibition period. Two important findings were presented in Figure 1A. First, a short inhibition period, which was commonly observed in RAFT and also PET-RAFT systems, depending on the amount of catalyst used was reduced with an increase of catalyst amount. Second, the polymerization kinetics are controlled by the amount of ZnTPP catalysts introduced into the system; an increase in catalyst concentration results in a subsequent increase of apparent propagation rate constants (k_p^{app}) (Figure 1A). The k_p^{app} gave k_p^{app} (blue) = 1.1×10^{-2} min^{-1}, 6.9×10^{-3} min^{-1} and 4.9×10^{-3} min^{-1} for different catalyst concentrations of 50, 10, and 5 ppm, respectively. However, increasing the catalyst concentration over 50 ppm did not promote the polymerization rates (Table S1, #6 versus #5) due to undesirable self-quenching of the photoredox catalyst which may include coupling of excitons, excimer formation, triplet−triplet annihilation, and dye−dye electron transfer.[113] The polymerization can be easily stopped by switching OFF the light and steadily restarted by switching ON (Figure 1B). Good agreement between the experimental and theoretical molecular weights was observed (Figure 1C), while the polydispersity decreased with monomer conversion, which is in perfect agreement with a living polymerization behavior.[114] In addition, polymerization under blue LED light maintained high end group fidelity as verified by NMR (SI, Figure S3). Further confirmation of end group fidelity of the synthesized homopolymers were demonstrated by successful chain extensions as discussed in Section 8. Finally, molecular weight distributions measured by GPC shifted symmetrically from low to high molecular weights during the polymerization (Figure 1D).

4. Polymerization under Red Light Irradiation Catalyzed by ZnTPP. ZnTPP shows remarkable properties in comparison to other photoredox catalysts that we have previously explored. In contrast to other catalysts such as *fac*-$[Ir(ppy)_3]$ and $Ru(bpy)_3Cl_2$, ZnTPP displayed several absorption signals, including a red-shifted minor absorption peak at 570 and 600 nm in DMSO. These absorption signals motivated us to carry out polymerization under red light. Polymerization of MA showed first-order kinetics for $\ln([M]_0/[M]_t)$ against exposure time with the propagation rate constant determined to be k_p^{app} (red) = 1.3×10^{-2} min^{-1} under red light

DOI: 10.1021/jacs.5b05274
J. Am. Chem. Soc. 2015, 137, 9174−9185

Table 3. Polymerization of Different Monomers by PET-RAFT Using ZnTPP with Various Thiocarbonylthio Compounds with 5 W red LEDs (λ_{max} = 635 nm) as a Light Source

#	exp. cond.[a] [M]:[RAFT]:[ZnTPP]	monomer	RAFT	[ZnTPP]/[M] (ppm)	time (h)	α[b] (%)	$M_{n,th.}$[c] (g/mol)	$M_{n,GPC}$[d] (g/mol)	M_w/M_n[d]
1[e]	200:0:1 × 10^{-3}	MA	–	50	2	10	–	–	–
2[f]	200:0:1 × 10^{-3}	MA	–	50	2	5	–	–	–
3[g]	200:1:1 × 10^{-3}	MA	BTPA	50	2	42	7460	6730	1.10
4[g]	200:1:1 × 10^{-3}	MA	BTPA	50	21	95	16 600	19 300	1.17
5[f]	200:1:1 × 10^{-3}	MA	BTPA	50	2	92	15 990	13 660	1.10
6[f]	200:1:2 × 10^{-2}	MA	BTPA	100	2	92	15 990	14 200	1.08
7[f]	200:1:1 × 10^{-3}	DMA	BTPA	50	2	95	18 300	19 200	1.04
8[f]	200:1:1 × 10^{-3}	NIPAM	BTPA	50	2	96	21 970	24 390	1.12
9[f]	200:1:1 × 10^{-3}	DMAEA	BTPA	50	2	42	12 300	14 300	1.36
10[f]	200:1:1 × 10^{-3}	Styrene	BTPA	50	18	28	6140	5000	1.19
11[f]	200:1:1 × 10^{-3}	Styrene	BSTP	50	18	31	6790	5700	1.40
12[f]	200:1:2 × 10^{-2}	HPMA	CDTPA	100	10	55	16 160	32 806	1.11

[a]The reactions were performed in the absence of oxygen at room temperature in dimethyl sulfoxide (DMSO). [b]Monomer conversion was determined by using ^{1}H NMR spectroscopy. [c]Theoretical molecular weight was calculated using the following equation: $M_{n,th.} = [M]_0/[RAFT]_0 \times MW^M \times \alpha + MW^{RAFT}$, where $[M]_0$, $[RAFT]_0$, MW^M, α, and MW^{RAFT} correspond to initial monomer concentration, initial RAFT concentration, molar mass of monomer, conversion determined by ^{1}H NMR, and molar mass of RAFT agent. [d]Molecular weight and polydispersity index (M_w/M_n) were determined by GPC analysis (DMAC as eluent) calibrated to polystyrene standard. [e]The reaction mixture was irradiated under 5 W blue LED light (λ_{max} = 460 nm). [f]The reaction mixture was irradiated under 5 W red LED light (λ_{max} = 635 nm). [g]The reactions were performed in the absence of oxygen at room temperature in *N*,*N*-dimethylformamide (DMF). Monomers: MA: methyl acrylate; DMA: *N*,*N*-dimethyl acrylamide; NIPAM: *N*-isopropylacrylamide; DMAEA: 2-(dimethylamino)ethyl acrylate; HPMA: *N*-(2-hydroxylpropyl) methacrylamide.

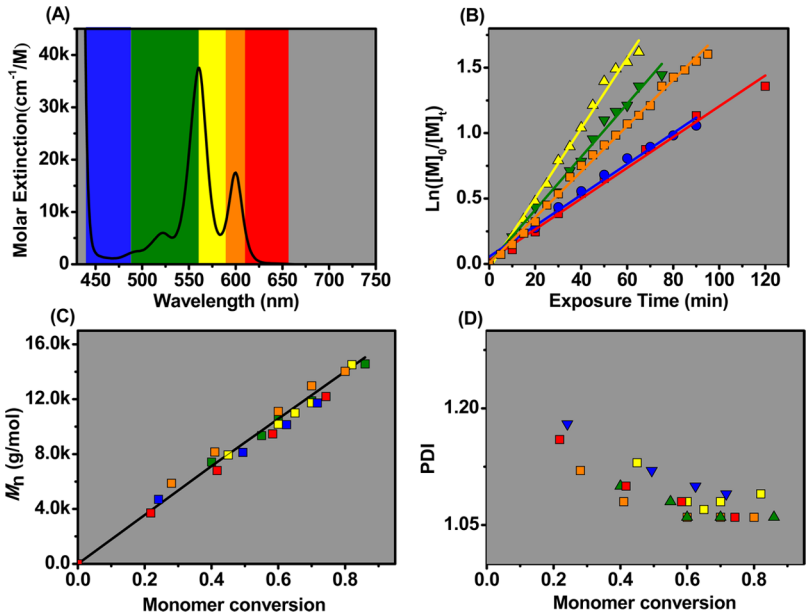

Figure 2. Polymerization under blue, green, yellow, orange and red lights using ZnTPP as the photoredox catalyst with [Monomer]:[RAFT]:[ZnTPP] = 200:1:1 × 10^{-2}. (A) Overlap of wavelength ranges of LED lights used on molar extinction spectrum of ZnTPP; (B) Plot of ln($[M]_0/[M]_t$) vs exposure time at catalyst concentration of 50 ppm; (C) M_n vs conversion; and (D) PDI vs conversion.

(Figure 3A). In the absence of BTPA, no monomer conversion was observed (Table 3, #2) leading to the assumption that direct monomer activation by catalyst was minimal for MA. In addition, a living polymerization was afforded by ZnTPP under red light irradiation as a linear relationship was observed for the plot of M_n against conversion as well as a decrease in molecular weight distributions with an increase in molecular weight (SI, Figure S4A,B). The polymerization can be temporally manipulated by switching "ON/OFF" the light source (SI, Figure 4C). Furthermore, polymerization under red LED light maintained high end group fidelity as verified with NMR (SI, Figure S5) by the presence of signal at 3.3 and 4.9 ppm attributed to Z group.

In order to test the versatility of this catalyst, polymerization under red light irradiation were performed in DMF, methanol and acetonitrile. Of these solvents, only *N*,*N*-dimethylformamide (DMF) afforded polymerization. Methanol and acetonitrile provided very low solubility of ZnTPP, and therefore, polymerization was not possible in these solvents. In the case of DMF, a slower polymerization was observed (Table 3, #3 and 4) in comparison to polymerization in DMSO (Table 3, #5 and 6). The slower polymerization can be attributed to coordination of the amide functionality on DMF to ZnTPP[115] which may hinder polymerization as it creates competition for thiocarbonylthio-Zn coordination.

DOI: 10.1021/jacs.5b05274
J. Am. Chem. Soc. 2015, 137, 9174–9185

Table 4. Polymerization of Methyl Acrylate under Different Wavelengths Using ZnTPP as Photoredox Catalyst (50 ppm Relative to Monomer) and BTPA as Thiocarbonylthio Compound

#	light	λ (nm)	k_p^{app} (min^{-1})	α (%)	$M_{n,th.}$[a] (g/mol)	$M_{n,GPC}$[b] (g/mol)	M_w/M_n[b]
1	blue	435−480	1.3×10^{-2}	70	12 300	13 000	1.08
2	green	480−560	2.0×10^{-2}	80	14 010	14 750	1.06
3	yellow	560−590	2.6×10^{-2}	82	14 360	14 500	1.09
4	orange	590−610	1.8×10^{-2}	84	14 700	13 100	1.08
5	red	610−655	1.2×10^{-2}	75	13 150	12 000	1.05

[a]Theoretical molecular weight was calculated using the following equation: $M_{n,th.} = [M]_0/[RAFT]_0 \times MW^M \times \alpha + MW^{RAFT}$, where $[M]_0$, $[RAFT]_0$, MW^M, α, and MW^{RAFT} correspond to initial monomer concentration, initial RAFT concentration, molar mass of monomer, conversion determined by ^1H NMR, and molar mass of RAFT agent. [b]Molecular weight and M_w/M_n were determined by GPC analysis (THF as eluent) calibrated to polystyrene standard.

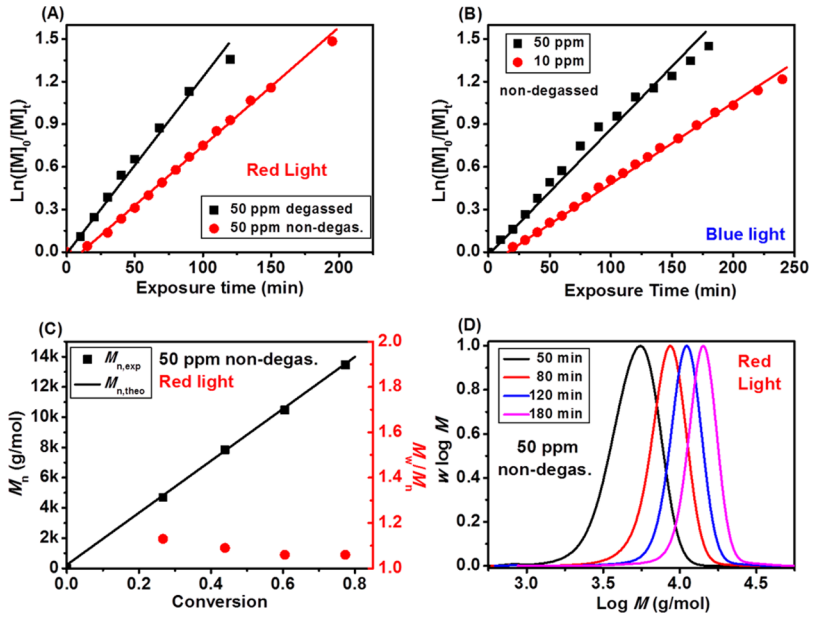

Figure 3. Kinetic study of PET-RAFT polymerization of MA with online Fourier transform near-infrared (FTNIR) measurement in the absence (degassed system) and presence (nondegassed system) of oxygen at room temperature with ZnTPP as the photoredox catalyst under red light irradiation with BTPA as the chain transfer agent, using molar ratio of [MA]:[BTPA] = 200:1 in DMSO. (A) Comparison plot of $\ln([M]_0/[M]_t)$ vs exposure time with catalyst concentration of 50 ppm in the presence and absence of oxygen under red light irradiation, (B) Comparison plot of $\ln([M]_0/[M]_t)$ vs exposure time with catalyst concentration of 50 and 10 ppm in the presence oxygen under blue light irradiation, (C) M_n vs conversion from (A) for 50 ppm nondegassed polymerization, and (D) molecular weight distributions at different time points from (C).

Tolerance of ZnTPP to other different monomer families (acrylamide, methacrylamide, styrene and vinyl acetate) and functionalities (including alcohol, tertiary amine, glycidyl, oligo(ethylene glycol) and isobornyl) were also tested (Table 3, #7−12 and SI, Table S2). Polymerization of *N*,*N*-dimethyl acrylamide (DMA) (Table 3, #7), *N*-isopropylacrylamide (NIPAM) (Table 3, #8) and *N*-(2-hydroxylpropyl) methacrylamide (HPMA) (Table 3, #12) yielded good control of molecular weight and molecular weight distributions. The experimental molecular weight of HPMA is slightly higher than the theoretical molecular weight due to the difference in hydrodynamic volume between HPMA and the linear PMMA standards used in DMAC GPC calibration.[116−119] In the case of 2-(dimethylamino)ethyl acrylate (DMAEA) (Table 3, #9), relatively high polydispersity was observed due to some possible side reactions between ZnTPP and monomers which may have led to higher events of termination. A similar scenario was also observed for the polymerization of styrene with BTPA (Table 3, #10) and benzylsulfanyl thiocarbonylthiosulfanyl propionic acid (BSTP) (Table 3, #11) where the molecular weight distributions for the latter were much higher than the former.

5. Controlling the Polymerization Rates by Tuning Light Wavelengths. As mentioned in the previous section, ZnTPP presents several absorption peaks at 422, 520, 570, and 600 nm (Figure 2A). We decided to investigate the polymerization kinetics of MA in the presence of BTPA as thiocarbonylthio compound and ZnTPP under other wavelengths (522, 565, and 595 nm which correspond to green, yellow, orange) (Figure 2A). The evolution of $\ln([M]_0/[M]_t)$ versus time in Figure 2B shows polymerization of MA proceeding rapidly in all these wavelengths. Interestingly, the polymerization rates depend strongly on the employed wavelength. The fastest to slowest polymerization rates (Table 4) are in the order of yellow > green > orange > red and blue. The slower polymerization rates in green light than yellow light was attributed to the emission of the green lamp which lies on the shoulder of the intense peak at 570 nm, while the emission of the yellow lamp is centered on the maximum absorption at 570 nm. Additionally, as the molar extinction coefficients are much lower in the red (~635 nm) and blue

DOI: 10.1021/jacs.5b05274
J. Am. Chem. Soc. 2015, 137, 9174−9185

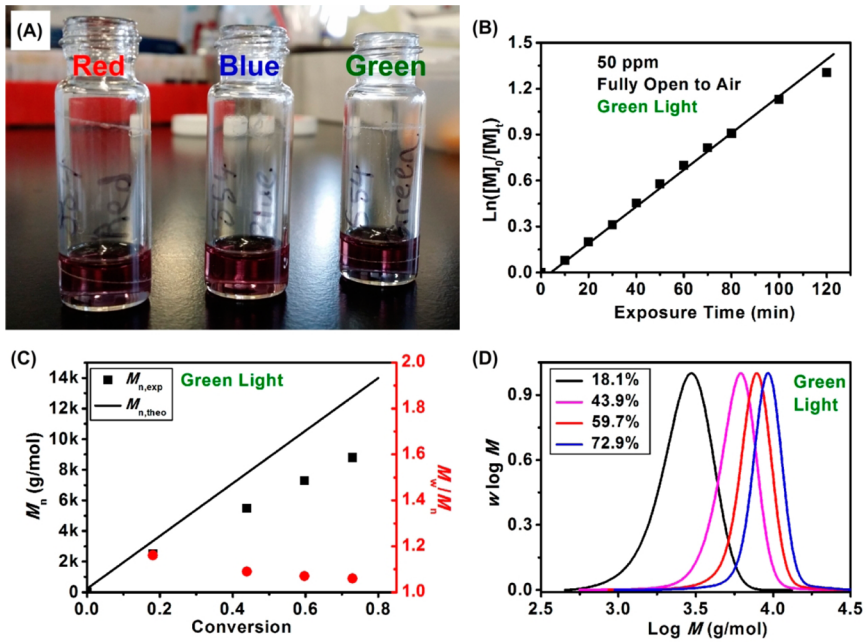

Figure 4. Polymerization of MA fully open to air at room temperature with ZnTPP as the photoredox catalyst under red light irradiation with BTPA as the chain transfer agent, using molar ratio of [MA]:[BTPA]:[ZnTPP] = 200:1:1× 10^{-3} in DMSO. (A) Picture of open glass vial reactors for different light reactions. (B) Kinetic plot of $\ln([M]_0/[M]_t)$ vs exposure time under green light irradiation. (C) M_n vs conversion for green light reaction, and (D) molecular weight distributions at different time points from (B).

regions (~460 nm), lower apparent propagation rate constants were observed. This is the first example, showing that a polymerization can be tuned by the wavelength using a single unique catalyst. In a previous work,[45] Goto, Kaji and co-workers have reported the polymerization of MMA under different wavelengths by using various photoredox catalysts. In our work, using a single photoredox catalyst, we were able to control the polymerization as demonstrated by the excellent control of the molecular weights in combination with the low polydispersity index (PDI < 1.10) (Figure 2C,D).

6. Comparative Study on Wavelength of Polymerization in the Presence and Absence of Oxygen. PET-RAFT polymerizations, using *fac*-[Ir(ppy)$_3$] and Ru(bpy)$_3$Cl$_2$ based catalysts, have been demonstrated to be tolerant to oxygen, as they can reduce oxygen to inactive species. To investigate the effects of oxygen in the case of ZnTPP, two polymerizations were carried out concurrently under red and blue lights, which correspond to the extreme parts of the visible spectrum. One reaction mixture was purged with nitrogen while the other was not. In red light (Figure 3A), a lower concentration of propagating radical (k_p^{app} (red) = 0.8 × 10^{-2} min^{-1}) was generated in the presence of oxygen (nondegassed system) as compared to the degassed system which had an apparent propagation rate constant of k_p^{app} (red) = 1.3 × 10^{-2} min^{-1}. However, we did not observe a substantial increase of the induction period in the presence of oxygen under red or blue light. Interestingly, the polymerization conducted by ZnTPP shows a significant difference in our early reports utilizing *fac*-[Ir(ppy)$_3$] and Ru(bpy)$_3$Cl$_2$, as photoredox catalysts[14,16] and other living radical polymerization techniques, where a substantial inhibition period was observed, including AGET and SET-LRP.[51,53,120−122] This result is attributed to the interaction between ZnTPP and trithiocarbonate, which allows direct activation of the PET-RAFT process without the need to reduce the oxygen. Repetition of this procedure with blue light in the presence of oxygen led to an observed apparent propagation rate constant of k_p^{app} (blue) = 0.8 × 10^{-2} min^{-1} (Figure 3B) which is much lower as compared to the degassed system (k_p^{app} (blue) = 1.1 × 10^{-2} min^{-1}) (Figure 1) for 50 ppm of catalyst. A lower apparent propagation rate constant was also observed for 10 ppm catalyst concentration (k_p^{app} (blue) = 0.6 × 10^{-2} min^{-1}) in comparison to 50 ppm catalyst concentration under blue (Figure 3B) and red (data not shown) light irradiation.

Polymerization in the presence and absence of oxygen maintained living characteristics with linear plots for M_n versus conversion, with an increase in the molecular weight and a decrease in the molecular weight distributions with conversion for both red (Figure 3C and 3D and SI, Figure S4) and blue (SI, Figure S6) lights. It is well-known that the presence of molecular oxygen, which has a radical-scavenging property, inhibits RAFT polymerization through early termination.[123] As the standard reduction potential of oxygen [E^{ϕ} (V) = −0.33] is much higher than the first reduction potential of the ZnTPP porphyrin ring (−1.31 V vs SCE in DMSO), it is also highly likely that the oxygen molecule can be reduced to hydroxide radical which will eventually be scavenged by DMSO.[14,124−126]

7. Controlled/"Living" Radical Polymerization Fully Open to Air. Encouraged by the results obtained for oxygen tolerance studies, we decided to push the boundaries of polymerization afforded by ZnTPP by conducting photopolymerization in vessels fully open to air. In this investigation, polymerization of MA mediated by ZnTPP (50 ppm relative to monomer concentration) was tested in open glass vials under three different lights, blue, green and red (Figure 4A). After 4 h light irradiation, the polymerization was stopped and aliquots were withdrawn for GPC and NMR measurements. Surprisingly, good control of molecular weight and molecular weight distributions (SI, Table S3) were obtained. However, the GPC molecular weights of the polymers for the different lights were much lower than the theoretical molecular weights due to monomer evaporation during the course of the polymerization.

DOI: 10.1021/jacs.5b05274
J. Am. Chem. Soc. 2015, 137, 9174−9185

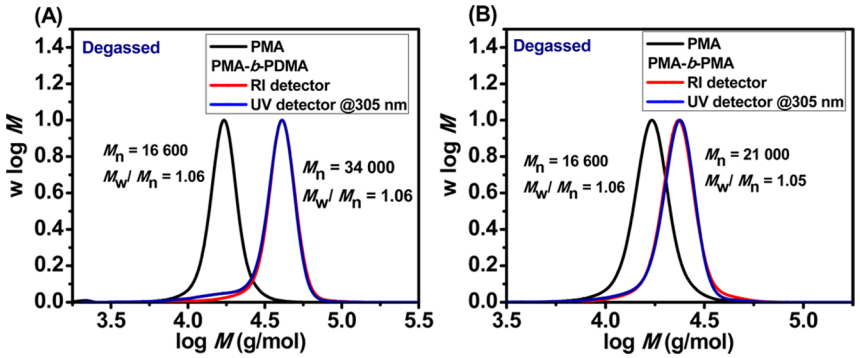

Figure 5. Molecular weight distributions for PMA macro-CTAs and their diblock copolymers synthesized under red light irradiation in the absence of air with ZnTPP as the catalyst and BTPA as the chain transfer agent at room temperature in DMSO: (A) PMA macro-CTA and PMA-*b*-PDMA (overlap of RI and UV signals after 1 h), and (B) PMA macro-CTA and PMA-*b*-PMA (overlap of RI and UV signals after 2 h).

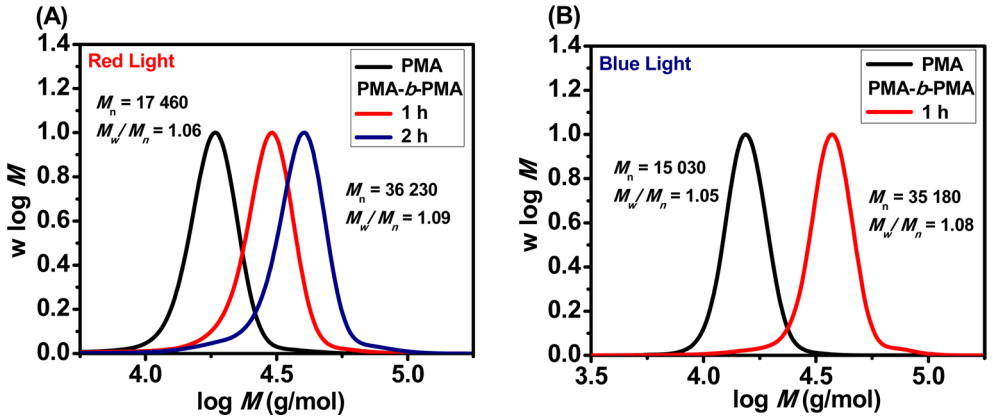

Figure 6. Molecular weight distributions for PMA macro-CTAs synthesized under blue and red LED lights in the presence of air and their diblock copolymers synthesized in the absence of air: (A) PMA macro-CTA and PMA-*b*-PMA in red light, and (B) PMA macro-CTA and PMA-*b*-PMA in blue light.

As the open vials are prone to monomer evaporation compared to vials sealed with septa, the calculation of the molecular weights based on monomer conversion is skewed.

Nevertheless, the controlled nature of the polymerization piqued our interest to further investigate the kinetics in an open air system. We employed the use of FTNIR to monitor the kinetics of MA polymerization under green light irradiation. Linear plot of $\ln([M]_0/[M]_t)$ versus exposure time indicated the presence of constant radical concentration in the reaction mixture (Figure 4B). Surprisingly, the polymerization proceeds in open air with no inhibition period. The molecular weight distributions remained low (M_w/M_n < 1.2) during the polymerization, although the experimental molecular weight was much lower than theoretical molecular weights due to unavoidable monomer evaporation in the open glass vials (Figure 4C). ^{1}H NMR analysis (SI, Figure S7) for final polymer products confirmed that not only the molecular weight assessed by NMR ($M_{n,NMR}$ = 8840 g/mol) was in good accord with GPC measurements ($M_{n,GPC}$ = 8790 g/mol), but also, demonstrated the presence of trithiocarbonate at the polymer end group. Judging from the symmetric GPC traces, with no observable shoulder and tailing, uinform polymer chain growth most likely occurred (Figure 4D). These results sufficiently support the uniqueness of ZnTPP as photoredox catalyst in activating PET-RAFT polymerization, which is mostly likely attributed to the selective interaction between ZnTPP and trithiocarbonate, and therefore, allowing direct activation of the PET-RAFT process in the presence of oxygen.

8. Chain Extension of Macromolecular Chain Transfer Agents (Macro-CTA) Synthesized in the Presence and Absence of Air. Chain extensions were carried out with PMA macro-CTA to investigate livingness of the synthesized homopolymers in the presence and absence of air. The synthesis of PMA macro-CTA was carried out in DMSO under blue and red light irradiation ($M_{n,GPC}$ = 16 600 g/mol, M_w/M_n = 1.06 and 70% monomer conversion for red light and $M_{n,GPC}$ = 14 300 g/mol, M_w/M_n = 1.06 and 62% monomer conversion for blue light) at a catalyst concentration of 50 ppm in the absence of air. After purification by precipitation, chain extension was carried out with MA and DMA monomers under the same light source used for macro-CTA synthesis with a molar ratio of [monomer]:[CTA]:[ZnTPP] = 500:1:2.5 × 10^{-2}. Macro-CTAs were successfully chain extended under red and blue LED lights with both MA and DMA monomers. Under red light irradiation (Figure 5), a complete shift in molecular weight of PMA macro-CTA was observed with the diblock copolymers having narrow molecular weight distributions ($M_{n,GPC,red}$ = 34 000 g/mol, M_w/M_n = 1.06 for PMA-*b*-PDMA in 1 h, and $M_{n,GPC,red}$ = 21 000 g/mol, M_w/M_n = 1.05 for PMA-*b*-PMA in 2 h). The UV and RI traces for both diblock copolymers showed good overlap which further confirmed the livingness of the system. Similar results were also obtained for chain extensions under blue light irradiation with MA and DMA monomers where diblocks with narrow molecular weight distributions (M_w/M_n < 1.10) were synthesized (SI, Figure S8).

DOI: 10.1021/jacs.5b05274
J. Am. Chem. Soc. 2015, 137, 9174−9185

In order the verify the livingness of the macro-CTAs synthesized in the presence of oxygen under blue and red light irradiation, chain extensions with MA were carried out (Figure 6). The synthesis of PMA macro-CTAs in an oxygenated system was carried out under blue and red light irradiation ($M_{n,GPC}$ = 17 460 g/mol, M_w/M_n = 1.06 and 89% monomer conversion for red light and $M_{n,GPC}$ = 15 030 g/mol, M_w/M_n = 1.05 and 86% monomer conversion for blue light) at a catalyst concentration of 50 ppm. These macro-CTAs were successfully chain extended in the absence of air with respect to the initial light used for their synthesis ($M_{n,GPC}$ = 36 230 g/mol, M_w/M_n = 1.09 for red light in 2 h and $M_{n,GPC}$ = 35 180 g/mol, M_w/M_n = 1.08 for blue light in 1 h at catalyst concentration of 50 ppm). The absence of shoulder at low molecular weight and low PDI demonstrates the absence (or low amount) of nonliving polymers.

9. Stability of ZnTPP under Light. The use of ZnTPP as photoredox catalyst for controlled/"living" radical polymerization has never been reported in the literature. As a consequence, this motivated us to investigate the stability of ZnTPP under prolonged exposure to light. Two glass vials with 50 ppm concentration of catalyst each were degassed before placing one vial in the dark while the other under red light irradiation for 16 h (SI, Figure S9). After 16 h, MA was added to the vial and degassed. Polymerizations were then carried out in the presence of BTPA with kinetics measured using online FTNIR on both samples. Interestingly, both preirradiated and control experiments (without preirradiation) for ZnTPP yielded the same propagation rate constants proving no significant degradation of ZnTPP upon prolonged irradiation.

In addition, the robustness of the ZnTPP catalyst can be demonstrated by successive chain extensions of PMA to generate a $P(MA)_5$ pentablock copolymer without supplementary addition of catalyst and repetitive purification steps. We first synthesized a PMA macro-CTA ($M_{n,GPC}$ = 9670 g/mol) by polymerization of MA in the presence of BTPA and 100 ppm of ZnTPP catalyst for 4 h in DMSO. NMR confirmed nearly full monomer conversion (>95%) in the first step. For the second block, MA in a degassed DMSO solution was then added under nitrogen to the macro-CTA, and the polymerization was allowed to continue for a further 6 h to reach full monomer conversion. This process was repeated three more times until the formation of the high-order pentablock polymers with high molecular weight ($M_{n,GPC} \approx$ 52 400 g/mol, $M_w/M_n \approx$ 1.21) was obtained. GPC analysis of the molecular weight distributions confirmed successful chain extensions as manifested by clear shifts to higher molecular weights in each step (Figure 7). The polymerization rates appear unchanged after these multiple chain extensions, which demonstrate that the catalyst is extremely stable under light.

CONCLUSIONS

Two major contributions to controlled/"living" radical polymerization were summarized in this study. First, we presented for the first time a photoinduced living polymerization activated by a new metalloporphyrin photoredox catalyst, ZnTPP, over a broad range of wavelengths (from 435 to 655 nm). The use of lower energy wavelength is an important step in the application of such photoinduced living polymerization technology for biomedical applications and materials sciences. Indeed, organic matter, including biological tissue and organic molecules presents a low absorption in red and NIR regions. Furthermore, in this contribution, we demonstrated that the polymerization rates could be easily manipulated by the use of a single unique photoredox catalyst over various visible wavelengths and temporally controlled by turning on/off the light. This finding would be useful for a variety of applications in the design of three-dimensional materials that require both spatial and temporal control.

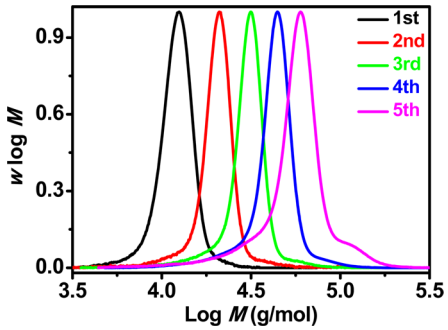

Figure 7. Molecular weight distribution of pentablock $P(MA)_5$ polymer synthesized by iterative addition of MA under red light irradiation in the presence of ZnTPP as catalyst and BTPA as chain transfer agent at room temperature in DMSO.

Second, it has always been a challenge to perform living radical polymerization in open air as oxygen is a radical scavenger that could rapidly trap propagating radicals. This contribution marks a step forward for controlled/living radical polymerization in a vessel fully open to air. In this study, ZnTPP acts as a photoredox catalyst that regulates living radical polymerization completely open to air without sacrificing living behavior. This result is most likely attributed to the unique and intriguing interaction between ZnTPP and trithiocarbonate, which will be the subject for further study in upcoming works.

ASSOCIATED CONTENT

Supporting Information

UV−vis spectra, NMR spectra, GPC traces. The Supporting Information is available free of charge on the ACS Publications website at DOI: 10.1021/jacs.5b05274.

AUTHOR INFORMATION

Corresponding Authors

*j.xu@unsw.edu.au
*cboyer@unsw.edu.au

Notes

The authors declare no competing financial interest.

ACKNOWLEDGMENTS

CB acknowledges Australian Research Council (ARC) for his Future Fellowship (F1200096) and thanks UNSW (DVCR Prof. Les Field) for internal funding (SPF01).

REFERENCES

(1) Kahn, K.; Plaxco, K. In *Recognition Receptors in Biosensors*; Zourob, M., Ed.; Springer: New York, 2010; pp 3−45.
(2) Baron, R.; McCammon, J. A. *Annu. Rev. Phys. Chem.* **2013**, *64*, 151−175.
(3) Woo, S.; Rothemund, P. W. K. *Nat. Chem.* **2011**, *3*, 620−627.
(4) Matyjaszewski, K.; Tsarevsky, N. V. *J. Am. Chem. Soc.* **2014**, *136*, 6513−6533.
(5) Hawker, C. J.; Bosman, A. W.; Harth, E. *Chem. Rev.* **2001**, *101*, 3661−3688.
(6) Moad, G.; Rizzardo, E.; Thang, S. H. *Chem. - Asian J.* **2013**, *8*, 1634−1644.

DOI: 10.1021/jacs.5b05274
J. Am. Chem. Soc. 2015, 137, 9174−9185

(7) Buchler, J. W. In *The Porphyrins*; Dolphin, D., Ed.; Academic Press: Waltham, MA, 1978; pp 389−483.
(8) Zhao, Y.; Yu, M.; Fu, X. *Chem. Commun.* **2013**, *49*, 5186−5188.
(9) Hsu, C.-S.; Yang, T.-Y.; Peng, C.-H. *Polym. Chem.* **2014**, *5*, 3867−3875.
(10) Zhao, Y.; Yu, M.; Zhang, S.; Liu, Y.; Fu, X. *Macromolecules* **2014**, *47*, 6238−6245.
(11) Peng, C.-H.; Li, S.; Wayland, B. B. *J. Chin. Chem. Soc.* **2009**, *56*, 219−233.
(12) Shanmugam, S.; Xu, J.; Boyer, C. *Chem. Sci.* **2015**, *6*, 1341−1349.
(13) Kang, J. S.; Kim, J.-S. *J. Biol. Chem.* **2000**, *275*, 8742−8748.
(14) Xu, J.; Jung, K.; Atme, A.; Shanmugam, S.; Boyer, C. *J. Am. Chem. Soc.* **2014**, *136*, 5508−5519.
(15) Shanmugam, S.; Xu, J.; Boyer, C. *Macromolecules* **2014**, *47*, 4930−4942.
(16) Xu, J.; Jung, K.; Boyer, C. *Macromolecules* **2014**, *47*, 4217−4229.
(17) Xu, J.; Jung, K.; Corrigan, N. A.; Boyer, C. *Chem. Sci.* **2014**, *5*, 3568−3575.
(18) Xu, J.; Shanmugam, S.; Duong, H. T.; Boyer, C. *Polym. Chem.* **2015**, DOI: 10.1039/C4PY01317D.
(19) Fu, C.; Xu, J.; Tao, L.; Boyer, C. *ACS Macro Lett.* **2014**, *3*, 633−638.
(20) Anastasaki, A.; Nikolaou, V.; Zhang, Q.; Burns, J.; Samanta, S. R.; Waldron, C.; Haddleton, A. J.; McHale, R.; Fox, D.; Percec, V.; Wilson, P.; Haddleton, D. M. *J. Am. Chem. Soc.* **2014**, *136*, 1141−1149.
(21) Anastasaki, A.; Nikolaou, V.; Simula, A.; Godfrey, J.; Li, M.; Nurumbetov, G.; Wilson, P.; Haddleton, D. M. *Macromolecules* **2014**, *47*, 3852−3859.
(22) Konkolewicz, D.; Schröder, K.; Buback, J.; Bernhard, S.; Matyjaszewski, K. *ACS Macro Lett.* **2012**, *1*, 1219−1223.
(23) Ribelli, T. G.; Konkolewicz, D.; Bernhard, S.; Matyjaszewski, K. *J. Am. Chem. Soc.* **2014**, *136*, 13303−13312.
(24) Ribelli, T. G.; Konkolewicz, D.; Pan, X.; Matyjaszewski, K. *Macromolecules* **2014**, *47*, 6316−6321.
(25) Xiao, P.; Dumur, F.; Zhang, J.; Gigmes, D.; Fouassier, J. P.; Lalevee, J. *Polym. Chem.* **2014**, *5*, 6350−6357.
(26) Kwak, Y.; Matyjaszewski, K. *Macromolecules* **2010**, *43*, 5180−5183.
(27) Pan, X.; Lamson, M.; Yan, J.; Matyjaszewski, K. *ACS Macro Lett.* **2015**, *4*, 192−196.
(28) Tasdelen, M. A.; Uygun, M.; Yagci, Y. *Macromol. Rapid Commun.* **2011**, *32*, 58−62.
(29) Tasdelen, M. A.; Uygun, M.; Yagci, Y. *Macromol. Chem. Phys.* **2010**, *211*, 2271−2275.
(30) Zhang, T.; Chen, T.; Amin, I.; Jordan, R. *Polym. Chem.* **2014**, *5*, 4790−4796.
(31) Yang, Q.; Dumur, F.; Morlet-Savary, F.; Poly, J.; Lalevée, J. *Macromolecules* **2015**, *48*, 1972−1980.
(32) Anastasaki, A.; Nikolaou, V.; McCaul, N. W.; Simula, A.; Godfrey, J.; Waldron, C.; Wilson, P.; Kempe, K.; Haddleton, D. M. *Macromolecules* **2015**, *48*, 1404−1411.
(33) Wenn, B.; Conradi, M.; Carreiras, A. D.; Haddleton, D. M.; Junkers, T. *Polym. Chem.* **2014**, *5*, 3053−3060.
(34) Chuang, Y.-M.; Ethirajan, A.; Junkers, T. *ACS Macro Lett.* **2014**, *3*, 732−737.
(35) Nikolaou, V.; Anastasaki, A.; Alsubaie, F.; Simula, A.; Fox, D. J.; Haddleton, D. M. *Polym. Chem.* **2015**, *6*, 3581−3585.
(36) Fors, B. P.; Hawker, C. J. *Angew. Chem., Int. Ed.* **2012**, *51*, 8850−8853.
(37) Fors, B. P.; Poelma, J. E.; Menyo, M. S.; Robb, M. J.; Spokoyny, D. M.; Kramer, J. W.; Waite, J. H.; Hawker, C. J. *J. Am. Chem. Soc.* **2013**, *135*, 14106−14109.
(38) Treat, N. J.; Fors, B. P.; Kramer, J. W.; Christianson, M.; Chiu, C.-Y.; Alaniz, J. R. d.; Hawker, C. J. *ACS Macro Lett.* **2014**, *3*, 580−584.
(39) Lalevée, J.; Tehfe, M.-A.; Dumur, F.; Gigmes, D.; Blanchard, N.; Morlet-Savary, F.; Fouassier, J. P. *ACS Macro Lett.* **2012**, *1*, 286−290.
(40) Versace, D.-L.; Cerezo Bastida, J.; Lorenzini, C.; Cachet-Vivier, C.; Renard, E.; Langlois, V.; Malval, J.-P.; Fouassier, J.-P.; Lalevée, J. *Macromolecules* **2013**, *46*, 8808−8815.
(41) Zhang, G.; Song, I. Y.; Ahn, K. H.; Park, T.; Choi, W. *Macromolecules* **2011**, *44*, 7594−7599.
(42) Chen, Y.; Hu, Z.; Xu, D.; Yu, Y.; Tang, X.; Guo, H. *Macromol. Chem. Phys.* **2015**, *216*, 1055−1060.
(43) Treat, N. J.; Sprafke, H.; Kramer, J. W.; Clark, P. G.; Barton, B. E.; Read de Alaniz, J.; Fors, B. P.; Hawker, C. J. *J. Am. Chem. Soc.* **2014**, *136*, 16096−16101.
(44) Shanmugam, S.; Xu, J.; Boyer, C. *Chem. Sci.* **2015**, *6*, 1341−1349.
(45) Ohtsuki, A.; Lei, L.; Tanishima, M.; Goto, A.; Kaji, H. *J. Am. Chem. Soc.* **2015**, *137*, 5610−5617.
(46) Chen, M.; MacLeod, M. J.; Johnson, J. A. *ACS Macro Lett.* **2015**, *4*, 566−569.
(47) Miyake, G. M.; Theriot, J. C. *Macromolecules* **2014**, *47*, 8255−8261.
(48) Ogawa, K. A.; Goetz, A. E.; Boydston, A. J. *J. Am. Chem. Soc.* **2015**, *137*, 1400−1403.
(49) Chen, M.; Johnson, J. A. *Chem. Commun.* **2015**, *51*, 6742−6745.
(50) Zhao, Y.; Yu, M.; Zhang, S.; Wu, Z.; Liu, Y.; Peng, C.-H.; Fu, X. *Chem. Sci.* **2015**, *6*, 2979−2988.
(51) Matyjaszewski, K.; Dong, H.; Jakubowski, W.; Pietrasik, J.; Kusumo, A. *Langmuir* **2007**, *23*, 4528−4531.
(52) Williams, V. A.; Ribelli, T. G.; Chmielarz, P.; Park, S.; Matyjaszewski, K. *J. Am. Chem. Soc.* **2015**, *137*, 1428−1431.
(53) Fleischmann, S.; Rosen, B. M.; Percec, V. *J. Polym. Sci., Part A: Polym. Chem.* **2010**, *48*, 1190−1196.
(54) Nguyen, N. H.; Percec, V. *J. Polym. Sci., Part A: Polym. Chem.* **2011**, *49*, 4756−4765.
(55) Zhang, Q.; Wilson, P.; Li, Z.; McHale, R.; Godfrey, J.; Anastasaki, A.; Waldron, C.; Haddleton, D. M. *J. Am. Chem. Soc.* **2013**, *135*, 7355−7363.
(56) Percec, V.; Guliashvili, T.; Ladislaw, J. S.; Wistrand, A.; Stjerndahl, A.; Sienkowska, M. J.; Monteiro, M. J.; Sahoo, S. *J. Am. Chem. Soc.* **2006**, *128*, 14156−14165.
(57) Nguyen, N. H.; Rosen, B. M.; Lligadas, G.; Percec, V. *Macromolecules* **2009**, *42*, 2379−2386.
(58) Mosnacek, J.; Eckstein-Andicsova, A.; Borska, K. *Polym. Chem.* **2015**, *6*, 2523−2530.
(59) Mosnáček, J.; Kundys, A.; Andicsová, A. *Polymers* **2014**, *6*, 2862−2874.
(60) Leibfarth, F. A.; Mattson, K. M.; Fors, B. P.; Collins, H. A.; Hawker, C. J. *Angew. Chem., Int. Ed.* **2013**, *52*, 199−210.
(61) Poelma, J. E.; Fors, B. P.; Meyers, G. F.; Kramer, J. W.; Hawker, C. J. *Angew. Chem., Int. Ed.* **2013**, *52*, 6844−6848.
(62) Yamago, S.; Ukai, Y.; Matsumoto, A.; Nakamura, Y. *J. Am. Chem. Soc.* **2009**, *131*, 2100−2101.
(63) Xiao, P.; Zhang, J.; Dumur, F.; Tehfe, M. A.; Morlet-Savary, F.; Graff, B.; Gigmes, D.; Fouassier, J. P.; Lalevée, J. *Prog. Polym. Sci.* **2015**, *41*, 32−66.
(64) Nakamura, Y.; Arima, T.; Tomita, S.; Yamago, S. *J. Am. Chem. Soc.* **2012**, *134*, 5536−5539.
(65) Muthukrishnan, S.; Pan, E. H.; Stenzel, M. H.; Barner-Kowollik, C.; Davis, T. P.; Lewis, D.; Barner, L. *Macromolecules* **2007**, *40*, 2978−2980.
(66) Liu, G.; Shi, H.; Cui, Y.; Tong, J.; Zhao, Y.; Wang, D.; Cai, Y. *Polym. Chem.* **2013**, *4*, 1176−1182.
(67) Khan, M. Y.; Cho, M.-S.; Kwark, Y.-J. *Macromolecules* **2014**, *47*, 1929−1934.
(68) Ohtsuki, A.; Goto, A.; Kaji, H. *Macromolecules* **2013**, *46*, 96−102.
(69) Tasdelen, M. A.; Çifct, M.; Uygun, M.; Yagci, Y. In *Progress in Controlled Radical Polymerization: Mechanisms and Techniques*; American Chemical Society: Washington, D.C., 2012; Vol. *1100*, pp 59−72.
(70) Shi, Y.; Liu, G.; Gao, H.; Lu, L.; Cai, Y. *Macromolecules* **2009**, *42*, 3917−3926.

DOI: 10.1021/jacs.5b05274
J. Am. Chem. Soc. 2015, 137, 9174−9185

(71) Zhang, H.; Deng, J.; Lu, L.; Cai, Y. *Macromolecules* **2007**, *40*, 9252−9261.
(72) Bansal, A.; Kumar, A.; Kumar, P.; Bojja, S.; Chatterjee, A. K.; Ray, S. S.; Jain, S. L. *RSC Adv.* **2015**, *5*, 21189−21196.
(73) Zhang, J.; Li, A.; Liu, H.; Yang, D.; Liu, J. *J. Polym. Sci., Part A: Polym. Chem.* **2014**, *52*, 2715−2724.
(74) Cao, Y.; Xu, Y.; Zhang, J.; Yang, D.; Liu, J. *Polymer* **2015**, *61*, 198−203.
(75) Kermagoret, A.; Wenn, B.; Debuigne, A.; Jerome, C.; Junkers, T.; Detrembleur, C. *Polym. Chem.* **2015**, *6*, 3847−3857.
(76) Anastasaki, A.; Nikolaou, V.; Brandford-Adams, F.; Nurumbetov, G.; Zhang, Q.; Clarkson, G. J.; Fox, D. J.; Wilson, P.; Kempe, K.; Haddleton, D. M. *Chem. Commun.* **2015**, *51*, 5626−5629.
(77) Zydziak, N.; Feist, F.; Huber, B.; Mueller, J. O.; Barner-Kowollik, C. *Chem. Commun.* **2015**, *51*, 1799−1802.
(78) Karatsu, T.; Yanai, M.; Yagai, S.; Mizukami, J.; Urano, T.; Kitamura, A. *J. Photochem. Photobiol., A* **2005**, *170*, 123−129.
(79) Zhang, S.; Li, B.; Tang, L.; Wang, X.; Liu, D.; Zhou, Q. *Polymer* **2001**, *42*, 7575−7582.
(80) Nagtegaele, P.; Galstian, T. V. *Synth. Met.* **2002**, *127*, 85−87.
(81) Tehfe, M.-A.; Lalevée, J.; Morlet-Savary, F.; Graff, B.; Blanchard, N.; Fouassier, J.-P. *Macromolecules* **2012**, *45*, 1746−1752.
(82) Lalevée, J.; Tehfe, M.-A.; Zein-Fakih, A.; Ball, B.; Telitel, S.; Morlet-Savary, F.; Graff, B.; Fouassier, J. P. *ACS Macro Lett.* **2012**, *1*, 802−806.
(83) Xiao, P.; Dumur, F.; Graff, B.; Gigmes, D.; Fouassier, J. P.; Lalevée, J. *Macromol. Rapid Commun.* **2013**, *34*, 1452−1458.
(84) Xiao, P.; Frigoli, M.; Dumur, F.; Graff, B.; Gigmes, D.; Fouassier, J. P.; Lalevée, J. *Macromolecules* **2014**, *47*, 106−112.
(85) Xiao, P.; Dumur, F.; Graff, B.; Fouassier, J. P.; Gigmes, D.; Lalevée, J. *Macromolecules* **2013**, *46*, 6744−6750.
(86) Tehfe, M.-A.; Lalevée, J.; Morlet-Savary, F.; Graff, B.; Fouassier, J.-P. *Macromolecules* **2011**, *44*, 8374−8379.
(87) Lu, L.; Zhang, H.; Yang, N.; Cai, Y. *Macromolecules* **2006**, *39*, 3770−3776.
(88) Shinokubo, H.; Osuka, A. *Chem. Commun.* **2009**, 1011−1021.
(89) Dolphin, D. In *The Porphyrins*; Dolphin, D., Ed.; Academic Press: Waltham, MA, 1978; p xv.
(90) Gust, D.; Moore, T. A.; Moore, A. L. *Acc. Chem. Res.* **2001**, *34*, 40−48.
(91) Collman, J.; Zhang, X.; Lee, V.; Uffelman, E.; Brauman, J. *Science* **1993**, *261*, 1404−1411.
(92) Lin, V.; DiMagno, S.; Therien, M. *Science* **1994**, *264*, 1105−1111.
(93) L. Anderson, H. *Chem. Commun.* **1999**, 2323−2330.
(94) Holten, D.; Bocian, D. F.; Lindsey, J. S. *Acc. Chem. Res.* **2002**, *35*, 57−69.
(95) Ethirajan, M.; Chen, Y.; Joshi, P.; Pandey, R. K. *Chem. Soc. Rev.* **2011**, *40*, 340−362.
(96) Sugimoto, H.; Kuroki, M.; Watanabe, T.; Kawamura, C.; Aida, T.; Inoue, S. *Macromolecules* **1993**, *26*, 3403−3410.
(97) Inoue, S.; Aida, T.; Watanabe, Y.; Kawaguchi, K.-I. *Makromol. Chem., Macromol. Symp.* **1991**, *42*−*43*, 365−371.
(98) Inoue, S.; Sugimoto, H.; Aida, T. *Macromol. Symp.* **1996**, *101*, 11−18.
(99) Simakova, A.; Mackenzie, M.; Averick, S. E.; Park, S.; Matyjaszewski, K. *Angew. Chem., Int. Ed.* **2013**, *52*, 12148−12151.
(100) Sigg, S. J.; Seidi, F.; Renggli, K.; Silva, T. B.; Kali, G.; Bruns, N. *Macromol. Rapid Commun.* **2011**, *32*, 1710−1715.
(101) Nguyen, K. A.; Day, P. N.; Pachter, R.; Tretiak, S.; Chernyak, V.; Mukamel, S. *J. Phys. Chem. A* **2002**, *106*, 10285−10293.
(102) Harriman, A. *J. Chem. Soc., Faraday Trans. 1* **1980**, *76*, 1978−1985.
(103) Harriman, A. *J. Chem. Soc., Faraday Trans. 2* **1981**, *77*, 1281−1291.
(104) Harriman, A. *J. Chem. Soc., Faraday Trans. 1* **1981**, *77*, 369−377.
(105) Fajer, J.; Borg, D. C.; Forman, A.; Dolphin, D.; Felton, R. H. *J. Am. Chem. Soc.* **1970**, *92*, 3451−3459.
(106) Pekkarinen, L.; Linschitz, H. *J. Am. Chem. Soc.* **1960**, *82*, 2407−2411.
(107) Seely, G. R. *Photochem. Photobiol.* **1978**, *27*, 639−654.
(108) Dreas-Wlodarczak, A.; Müllneritsch, M.; Juffmann, T.; Cioffi, C.; Arndt, M.; Mayor, M. *Langmuir* **2010**, *26*, 10822−10826.
(109) Uchiyama, M.; Satoh, K.; Kamigaito, M. *Angew. Chem., Int. Ed.* **2015**, *54*, 1924−1928.
(110) Kumagai, S.; Nagai, K.; Satoh, K.; Kamigaito, M. *Macromolecules* **2010**, *43*, 7523−7531.
(111) Aoshima, H.; Uchiyama, M.; Satoh, K.; Kamigaito, M. *Angew. Chem., Int. Ed.* **2014**, *53*, 10932−10936.
(112) Xu, J.; Shanmugam, S.; Corrigan, N. A.; Boyer, C. In *Controlled Radical Polymerization: Mechanisms*; American Chemical Society: Washington, D.C., 2015; Vol. *1187*, pp 247−267.
(113) Konishi, T.; Ikeda, A.; Asai, M.; Hatano, T.; Shinkai, S.; Fujitsuka, M.; Ito, O.; Tsuchiya, Y.; Kikuchi, J.-I. *J. Phys. Chem. B* **2003**, *107*, 11261−11266.
(114) Goto, A.; Fukuda, T. *Prog. Polym. Sci.* **2004**, *29*, 329−385.
(115) Nappa, M.; Valentine, J. S. *J. Am. Chem. Soc.* **1978**, *100*, 5075−5080.
(116) Teodorescu, M.; Matyjaszewski, K. *Macromolecules* **1999**, *32*, 4826−4831.
(117) Teodorescu, M.; Matyjaszewski, K. *Macromol. Rapid Commun.* **2000**, *21*, 190−194.
(118) Nguyen, N. H.; Rodriguez-Emmenegger, C.; Brynda, E.; Sedlakova, Z.; Percec, V. *Polym. Chem.* **2013**, *4*, 2424−2427.
(119) Senoo, M.; Kotani, Y.; Kamigaito, M.; Sawamoto, M. *Macromolecules* **1999**, *32*, 8005−8009.
(120) Min, K.; Jakubowski, W.; Matyjaszewski, K. *Macromol. Rapid Commun.* **2006**, *27*, 594−598.
(121) McMahon, J. J.; Barry, M.; Breen, K. J.; Radziwon, A. K.; Brooks, L. D.; Blair, M. R. *J. Phys. Chem. C* **2008**, *112*, 1158−1166.
(122) Wang, G.; Lu, M.; Wu, H. *Polym. Bull.* **2012**, *69*, 417−427.
(123) Gody, G.; Barbey, R.; Danial, M.; Perrier, S. *Polym. Chem.* **2015**, *6*, 1502−1511.
(124) Rosenblum, W. I.; El-Sabban, F. *Stroke* **1982**, *13*, 35−39.
(125) Valko, M.; Izakovic, M.; Mazur, M.; Rhodes, C. J.; Telser, J. *Mol. Cell. Biochem.* **2004**, *266*, 37−56.
(126) Kadish, K. M.; Davis, D. G. *Ann. N. Y. Acad. Sci.* **1973**, *206*, 495−503.

DOI: 10.1021/jacs.5b05274
J. Am. Chem. Soc. 2015, 137, 9174−9185